

# Curing Reaction of Epoxy Resins with Diamines

C. C. RICCARDI, H. E. ADABBO, and R. J. J. WILLIAMS,\* *Institute of Materials Science and Technology (INTEMA), University of Mar del Plata and National Research Council (CONICET), (7600) Mar del Plata, Argentina*

## Synopsis

The curing reaction of a commercial bisphenol A diglycidyl ether (BADGE) with ethylenediamine (EDA) was studied by differential scanning calorimetry. Different kinetic expressions were found with isothermal (low temperature range) and dynamic (high temperature range) runs. Two competitive mechanisms are shown to be present: an autocatalytic one (activation energy  $E = 14$  kcal/mol) and a noncatalytic path characterized by a second-order reaction with  $E = 24.5$  kcal/mol. At low temperatures both mechanisms took place simultaneously, showing a significant decrease in the reaction rate after the gel point. At high temperatures only the noncatalytic reaction was present, without showing a noticeable rate decrease in the rubber region. Also, a third-order dependence of the glass transition temperature on reaction extent is shown.

## INTRODUCTION

The mechanism and kinetics of the curing reaction of epoxy resins with diamines has been analyzed and reviewed by several investigators.<sup>1-7</sup> The following aspects of the reaction are well established in the literature: both hydrogen atoms of the amino group take place successively in the addition reaction



Although both reaction rates may be different, experimental data are consistent with a single activation energy and reaction heat for both steps. Other possible reactions, namely, the homopolymerization of epoxy groups or its reaction with hydroxyl functionalities, can be neglected under certain curing conditions.

—Isothermal runs show an increase in the reaction rate due to the catalytic effect of the hydroxyl groups generated in the reaction. The activation energy of this autocatalytic reaction is close to 54–59 kJ/mol (13–14 kcal/mol).

—The ratio of primary and secondary amino groups reactivities may vary with the particular diamine used.

—The curing reaction may be quenched, at least for practical purposes, if the system vitrifies at a particular reaction extent.<sup>8</sup>

\* To whom all correspondence should be addressed.



range  $10^5$ – $4.5 \times 10^6$  Pa (14.7–650 psi), using known values of the heat capacity of alumina and heat of fusion of indium. The curing in the scanning mode was conducted at  $4.5 \times 10^6$  Pa, under nitrogen, using different heating rates: 5, 10, and  $20^\circ\text{C}/\text{min}$ . Isothermal runs were performed as follows. The pressure cell was stabilized, without the cover, at the required temperature. The sample, contained in a closed capsule, was positioned and the run started. This procedure avoided the premature curing which took place during the stabilization period when the sample was placed before the initial heating up. The temperature range for isothermal runs was limited to  $40$ – $60^\circ\text{C}$ . At lower temperatures the DSC signal had not enough intensity to get accurate results. At higher temperatures a significant reaction extent took place during the signal perturbation produced with the sample introduction.

**Glass Transition.** Samples were cured for prolonged periods (i.e., more than 24 h) at constant temperature. For temperatures higher than  $35^\circ\text{C}$  the reaction was performed in the DSC pressure cell. For lower temperatures, the cell shown in Figure 1 was used. It consisted of two copper plaques supported on teflon discs which were separated by a rubber *o*-ring. The gap for the sample had 2.5 mm thickness. The desired temperature was attained with an ethanol–water mixture circulating from a cryostat. Both the glass transition  $T_g$  and the residual reactivity of the cured samples were determined in the thermal analyzer at a  $10^\circ\text{C}/\text{min}$  heating rate.

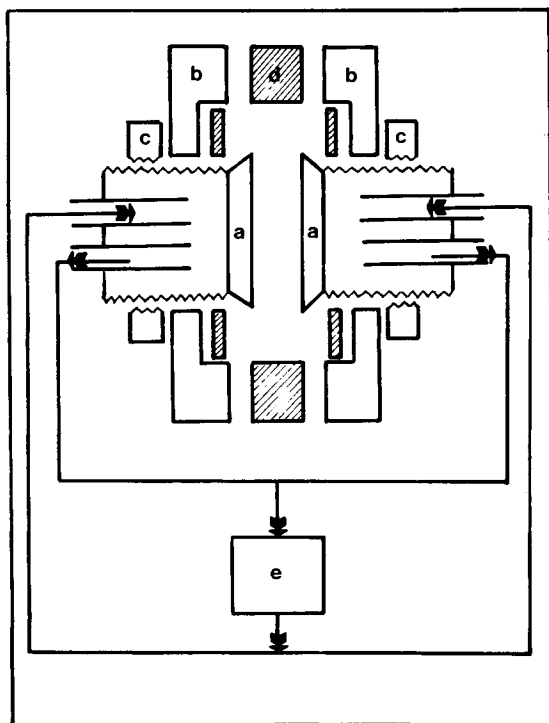


Fig. 1. Device for curing samples at low temperatures: (a) copper plaques, 50 mm  $\phi$ , 5 mm thickness; (b) Teflon discs; (c) aluminum discs; (d) rubber *o*-ring; (e) cryostat.

## RESULTS AND DISCUSSION

## Kinetics

Figure 2 shows four dynamic runs carried out at three different heating rates. From the total area under the curves the following heat of reaction was obtained

$$\Delta H_T = 524 \text{ kJ/kg} = 23.5 \text{ kcal/eq}$$

This value agrees satisfactorily with results reported for the reaction of phenyl glycidyl ether with butylamine, taken as a model system<sup>1</sup> ( $\Delta H_T = 24.5 \pm 0.6 \text{ kcal/eq}$ ). Thus, it may be concluded that scanning runs lead to a complete reaction extent.

The kinetics of the curing reaction under the scanning mode was obtained from the DSC information using the classic Barrett's method.<sup>16</sup> If the kinetic equation is written in terms of the conversion  $x = \Delta H/\Delta H_T$  (ratio of the heat evolved up to a certain temperature over total reaction heat), as

$$dx/dt = Af(x) \exp(-E_A/RT), \quad (3)$$

then

$$\ln[(dx/dt)/f(x)] = \ln k = \ln A - E_A/RT \quad (4)$$

A plot of  $\ln k$  vs.  $1/T$  will be linear if  $f(x)$  is correctly chosen. Figure 3 shows such a plot for  $f(x) = (1 - x)^2$  and three different heating rates. Each run gives a good correlation over the whole conversion range. However, increasing the heating rate leads to a lower preexponential factor  $A$ ,

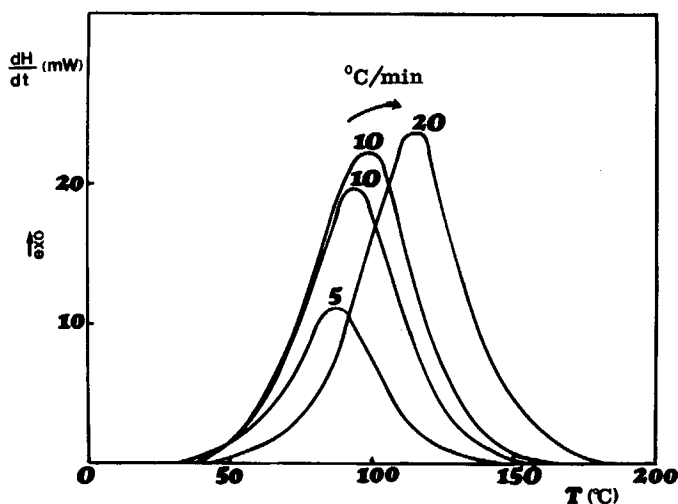


Fig. 2. Curing of the epoxy resin with ethylenediamine using the dynamic mode of the DSC, at different heating rates.

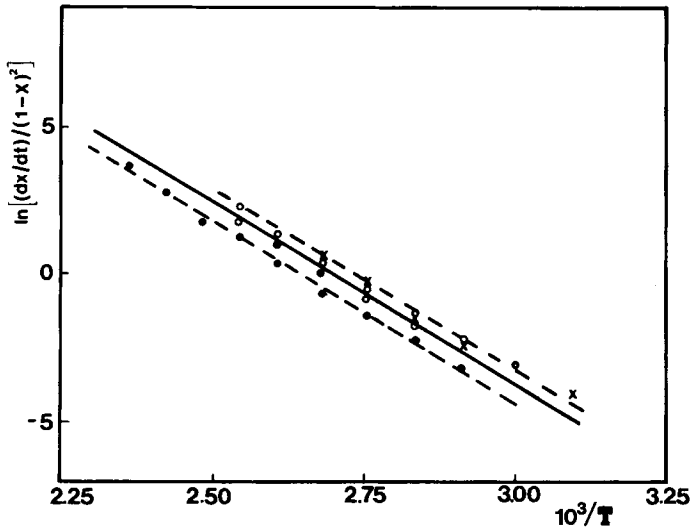


Fig. 3. Linear regression of dynamic DSC runs using Barrett's technique. (x) 5°C/min; (O) 10°C/min; (●) 20°C/min.

but the same activation energy  $E_A$ . In order to take a reliable average  $A$  value, a simultaneous correlation of 20 experimental runs carried out at the three different heating rates was performed. The following kinetic expression was obtained:

$$dx/dt \text{ (s}^{-1}\text{)} = 4.5 \times 10^{12} \exp(-12330/T)(1-x)^2 \tag{5}$$

The activation energy is  $E_A = 102.6 \text{ kJ/mol} = 24.5 \text{ kcal/mol}$ . Equation (5) is depicted with a full line in Figure 3. The dotted lines show the maximum variation of the preexponential factor. The resulting range is  $A = 2.3 - 6.9 \times 10^{12} \text{ s}^{-1}$ . This is believed to be more the result of the thermal response of the calorimeter than a problem associated to the reaction itself.

The validity of eq. (5) may be verified by comparing its integral expression with the experimental  $x$  vs.  $T$  results, for different heating rates. As Barrett's method uses both the rate  $dx/dt$  and the conversion  $x$  at every temperature, and the integral method does only need the conversion, this last one may be regarded as an independent verification of the proposed kinetic equation. Thus, if  $q = dT/dt$  is the constant heating rate,

$$\int_0^x \frac{dx}{(1-x)^2} = \frac{4.5 \times 10^{12}}{q} \int_{T_0}^T \exp(-12330/T) dT \tag{6}$$

By calling  $z = 12330/T$ ,  $dz = -z^2 dT/12330$ , eq. (6) may be written as

$$x/(1-x) = - [3.33 \times 10^{18}/q \text{ (}^\circ\text{C/min)}] \int_{z_0}^z [\exp(-z)/z^2] dz \tag{7}$$

For  $z > 15$ , which covers the actual curing range, the integral

$$F(z) = - \int_0^z [\exp(-z/z^2)] dz \quad (8)$$

may be calculated as<sup>17</sup>

$$\ln F(z) = - 5.330 - 1.0516z \quad (9)$$

Then,

$$\begin{aligned} x/(1-x) &= [1.61 \times 10^{16}/q \text{ (}^\circ\text{C/min)}] \\ &[\exp(-12966/T) - \exp(-12966/T_0)] \end{aligned} \quad (10)$$

For runs started at room temperature, the last exponential does not contribute significantly. Then,

$$\ln[qx \text{ (}^\circ\text{C/min)} / 1.61 \times 10^{16}(1-x)] = - 12966/T \quad (11)$$

Figure 4 shows a plot of eq. (11) for three different heating rates, confirming the reasonable accuracy of the proposed second order kinetic equation. As in Figure 3, the plotted runs show the maximum dispersion range (points for the other 16 runs are included in this range).

Figure 5 shows three typical isothermal runs. Now the kinetics is clearly autocatalytic, and agrees in general trends with results reported by Horie et al. for the same system.<sup>1</sup>

In order to give an interpretation to both isothermal and dynamic results, the following kinetic model is postulated:

I. The reactivity of primary ( $k_1$ ) and secondary ( $k_2$ ) amino hydrogens in EDA is almost the same (Horie et al.<sup>1</sup> postulated a ratio  $k_2/k_1 = 1.2$ ).

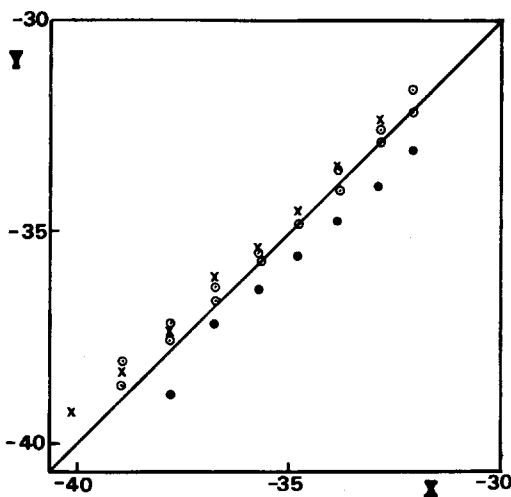


Fig. 4. Verification of the second order kinetic equation using an integral method  $\{ Y = \ln[qx/1.61 \times 10^{16}(1-x)]; X = -12,966/T \}$ : (x) 5°C/min; (O) 10°C/min; (●) 20°C/min.

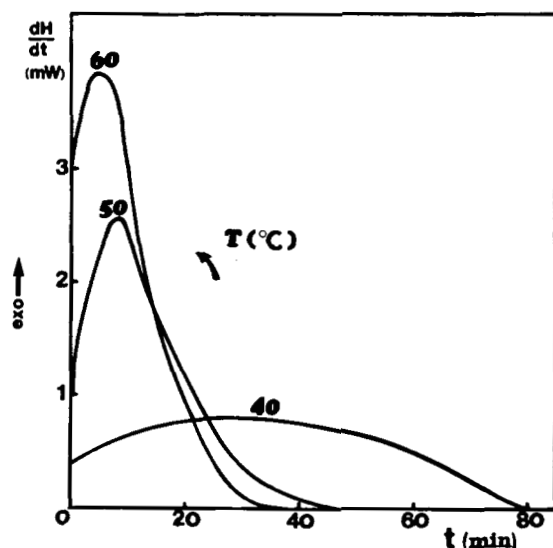


Fig. 5. Isothermal DSC runs.

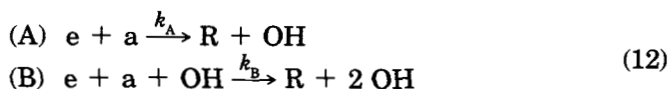
II. The reaction takes place by two competitive paths; one is catalyzed by the hydroxyls initially present in BADGE and those generated during the reaction, and the other is a noncatalytic mechanism with a higher activation energy.

III. The catalytic mechanism vanishes at high temperatures (temperature range of dynamic runs); this may be based on the difficulty of forming the ternary transition complex.<sup>1</sup>

IV. The noncatalytic reaction takes place over all the temperature range.

Under the previous hypotheses, the noncatalytic reaction has a second order dependence on concentration and an activation energy  $E_A = 102.6$  kJ/mol = 24.5 kcal/mol [eq. (5)].

In the low temperature range (isothermal runs) both mechanisms occur simultaneously:



where  $e$  = epoxy group,  $a$  = amino hydrogen, A = noncatalytic reaction, and B = catalytic mechanism.

The consumption of epoxy groups is given by

$$-de/dt = [k_A + k_B(\text{OH})]ea
 \tag{13}$$

For stoichiometric mixtures,

$$e = a = e_0(1 - x) \quad \text{and} \quad (\text{OH}) = (\text{OH})_0 + e_0x.$$

Then,

$$dx/dt = (k_A e_0 + k_B e_0 (\text{OH})_0 + k_B e_0^2 x) (1 - x)^2
 \tag{14}$$

Figure 6 shows a plot of  $(dx/dt)/(1-x)^2$  vs.  $x$  for the three temperatures. The agreement is satisfactory up to conversions close to the gel point ( $x_g = 0.577$ ). At this conversion the catalytic mechanism is much more important than the noncatalytic one. The significant decrease in the reaction rate after passing the gel conversion, may be attributed to the difficulty in forming the  $e-a-OH$  transition complex due to diffusional restrictions. This effect was already shown by Horie et al.<sup>1</sup> When EDA is replaced by longer diamines such as HMDA (hexamethylenediamine), the decrease in the reaction rate is observed at higher conversions.<sup>1,6</sup> In this case the deceleration may be tied to the overall diffusion control due to entering the glass transition region. In every case, the reaction ceases before complete conversion is attained due to vitrification (see following section).

It is possible to compare our results with those of Horie et al.<sup>1</sup> for the same system. The best regression of the slopes plotted in Figure 6 gives

$$k_B = 2.17 \times 10^5 \exp(-7060/T) \quad (L^2/\text{eq}^2 \cdot \text{s}) \quad (15)$$

Then, the activation energy of the catalytic reaction is  $E_B = 58.6$  kJ/mol = 14.0 kcal/mol. This value is in excellent agreement with all the available information concerning the epoxy-amine reaction at low temperatures (isothermal runs). Table I shows a comparison between our results and those of Horie et al.<sup>1</sup> The agreement is reasonable considering that minor changes in the calorimeters calibration would account for the observed differences.

The reliability of the proposed kinetic model may now be tested by comparing the observed initial reaction rate with the one predicted by eq.(14) From eq. (5),

$$k_A e_0 = 2.7 \times 10^{14} \exp(-12330/T) \quad (\text{min}^{-1})$$

Also, from eq. (15) with  $e_0 = 5.84$  eq/L and  $(OH)_0 = 0.061e_0$  ( $n = 0.122$  in Badge's structural formula—Experimental section),

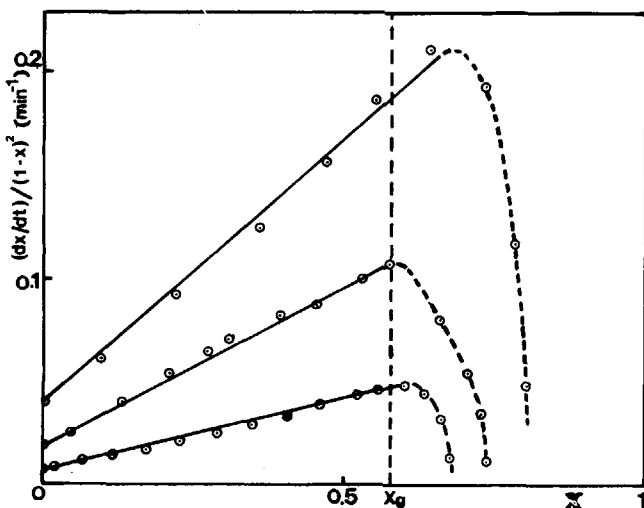


Fig. 6. Linear regression of isothermal DSC runs using the proposed kinetic model.

TABLE I  
Values of the Autocatalytic Rate Constant  $k_B$

$T$ (°C)	$k_B$ (L <sup>2</sup> /eq <sup>2</sup> · s)	
	This paper	Horie et al. <sup>1</sup>
50	$0.70 \times 10^{-4}$	$0.52\text{--}0.57 \times 10^{-4}$
60	$1.35 \times 10^{-4}$	$1.10 \times 10^{-4}$
70	$2.50 \times 10^{-4a}$	$1.90 \times 10^{-4}$

<sup>a</sup> Extrapolated from Eq. (15).

$$k_B e_0(\text{OH})_0 = 2.71 \times 10^7 \exp(-7060/T) \quad (\text{min}^{-1})$$

Then,

$$(dx/dt)_0 = k_A e_0 + k_B e_0(\text{OH})_0 \quad (16)$$

Table II shows an excellent agreement between experimental and predicted values, confirming the reliability of the proposed kinetic model.

Then, the reaction between epoxies and amines is characterized by two competitive mechanisms: the noncatalytic one, with an activation energy  $E = 24.5$  kcal/mol, takes place over all the temperature range; the autocatalytic one, with an activation energy  $E = 14.0$  kcal/mol, is significant at low temperatures but vanishes at high temperatures (due to the difference in activation energies the contribution of the catalytic mechanism decreases with increasing temperature; however, it would have still been significant in the temperature range of dynamic runs if its disappearance as an alternative reaction path had not been accepted). When the reaction takes place in the rubbery region (after the gel point), a significant decrease in the rate of the catalytic path is observed while the noncatalytic reaction is not affected (at least in the temperature range of dynamic runs). The restrictions to carry out the catalytic reaction in the rubbery region may be associated with steric hindrances for the simultaneous approach of epoxy, amine, and hydroxyl groups which are joined to the gel. This effect is particularly noteworthy with short diamines such as EDA.

With these results, the open questions remaining in the related literature may be answered. The serious disagreement between programmed heating rate and isothermal experiments is a direct consequence of having two possible reaction paths, with different kinetic parameters, and with relative importance depending on the temperature range. A similar phenomenon

TABLE II  
Experimental and Predicted Values of the Initial Reaction Rate

$T$ (°C)	Experimental (min <sup>-1</sup> ) $(dx/dt)_0$	Predicted (min <sup>-1</sup> )			=	$(dx/dt)_0$
		$k_A e_0$	+	$k_B e_0(\text{OH})_0$		
40	0.0060	0.0021		0.0043		0.0064
50	0.0160	0.0071		0.0087		0.0158
60	0.0400	0.0224		0.0168		0.0392

has been shown in the curing of an unsaturated polyester with styrene.<sup>18</sup> Also, the decrease of the reaction rate in the rubbery region is not observed in dynamic runs because the effect does not apply to the noncatalytic reaction path.

### Glass Transition

Figure 7 shows a typical scan at 10°C/min after an isothermal curing at  $T = 60^\circ\text{C}$ , leading to the vitrification of the sample. The glass transition always appeared at a temperature 15°C higher than the curing temperature. This effect is typical of the scanning method involved in the measurement of  $T_g$ . From the residual enthalpy ( $\Delta H_R$ ) the conversion attained in the isothermal curing could be calculated. The resulting conversion vs. curing temperature curve, associated with vitrification, is shown in the phase diagram plotted in Figure 8. The vitrification curve improves previous results for the same system,<sup>1</sup> taken on the basis of an apparent final conversion for isothermal runs.

The increase in the glass transition arises from an increase in molecular weight, branching, and crosslinking density (after the gel point). Experimental data are reasonably correlated with the following equation:

$$T_g (\text{°C}) = -14 + 94x^3 \quad (17)$$

The value of  $T_{g\infty} = 80^\circ\text{C}$ , arising from eq. (17) could not be checked with fully cured samples due to the low sensitivity of the  $T_g$  signal in these samples.

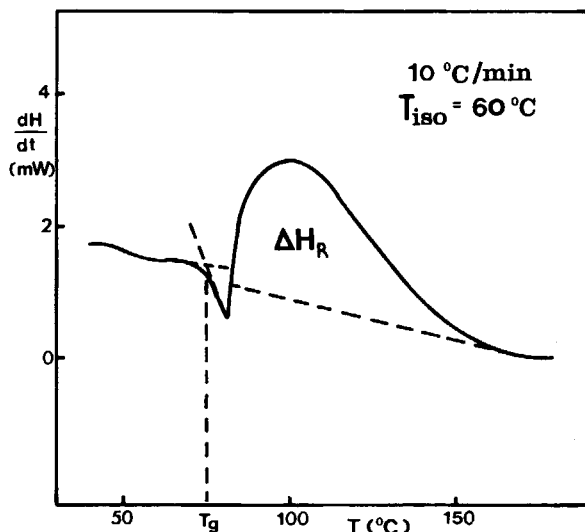


Fig. 7. Scan at 10°C/min after an isothermal curing at 60°C for 24 h.

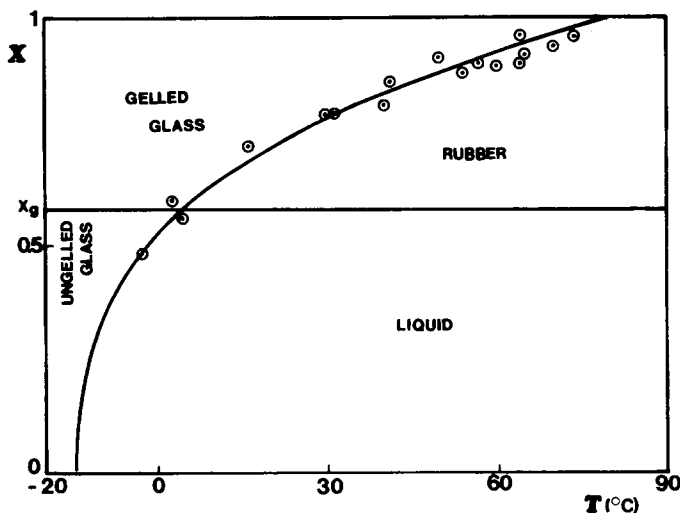


Fig. 8. Phase diagram for the BADGE ( $n = 0.122$ )-EDA system.

### CONCLUSIONS

Analysis of the reaction between BADGE and EDA, taken as a model system for the curing of epoxy resins with diamines, showed the following facts:

—The curing proceeds by two competitive mechanisms: an autocatalytic one characterized by an activation energy  $E_B = 14$  kcal/mol, and a noncatalytic path identified by a second order reaction with an activation energy  $E_A = 24.5$  kcal/mol.

—At low temperatures (range of DSC isothermal runs) both mechanisms take place simultaneously. However, in the rubber region at least the autocatalytic path is severely retarded. This effect is less significant with longer diamines.<sup>1,6</sup>

—At high temperatures (range of DSC dynamic runs) the reaction follows the noncatalytic mechanism. The autocatalytic path is no longer a valid alternative, possibly due to the difficulty in the formation of the ternary transition complex.<sup>1</sup> Gelation does not show any effect over the noncatalytic reaction rate.

—The different kinetic expressions obtained with isothermal and dynamic DSC runs, for other epoxy-diamine systems<sup>2,13</sup> may be now explained on the basis of a change of mechanism with curing temperature. Alternative arguments, such as the necessity of using dynamic rate equations,<sup>11-13</sup> have shown to be inconsistent.<sup>14</sup>

The authors wish to thank both the financial support and a scholarship given to C. C. R. by the Comisión de Investigaciones Científicas de la Provincia de Buenos Aires. The financial support provided by the Subsecretaría de Ciencia y Tecnología, Argentina, is also acknowledged. Ciba-Geigy Argentina has kindly supplied the Araldit GY 250 for this study.

## References

1. K. Horie, H. Hiura, M. Sawada, I. Mita, and H. Kambe, *J. Polym. Sci., A-1*, **8**, 1357 (1970).
2. R. B. Prime, *Polym. Eng. Sci.*, **13**, 365 (1973).
3. M. R. Kamal, S. Sourour, and M. Ryan, *Soc. Plast. Eng. Tech. Pap.*, **19**, 187 (1973).
4. V. A. Erä and A. Mattila, *J. Therm. Anal.*, **10**, 461 (1976).
5. K. Dušek, M. Ilavský, and S. Luňák, *J. Polym. Sci., Polym. Symp.*, **53**, 29 (1976).
6. S. Luňák and K. Dušek, *J. Polym. Sci., Polym. Symp.*, **53**, 45 (1976).
7. S. Luňák, J. Vladyka, and K. Dušek, *Polymer*, **19**, 931 (1978).
8. H. E. Adabbo and R. J. J. Williams, *J. Appl. Polym. Sci.*, **27**, 1327 (1982).
9. M. Cizmeociogly and A. Gupta, *SAMPE Q.*, **13**(Apr) (1982).
10. A. Dutta and M. E. Ryan, *J. Appl. Polym. Sci.*, **24**, 635 (1979).
11. J. P. McCallum and J. Tanner, *Nature*, **225**, 1127 (1970).
12. A. L. Draper, *Proceedings of the Third Symposium on Thermal Analysis*, Toronto University Press, Toronto, 1970, p. 63.
13. R. B. Prime, *Anal. Calorimetry*, **2**, 201 (1970).
14. J. Sesták, *J. Thermal Anal.*, **16**, 503 (1979).
15. J. Urbansky, W. Czerwinski, K. Janicka, F. Majewska, and H. Zowall, *Handbook of Analysis of Synthetic Polymers and Plastics*; Ellis Horwood, Chichester, and Wydawnictwa Naukowo-Techniczne, Warsaw, 1977, p. 302.
16. K. E. J. Barrett, *J. Appl. Polym. Sci.*, **11**, 1617 (1967).
17. T. Ozawa, *J. Thermal Anal.*, **2**, 301 (1970).
18. T. R. Cuadrado, J. Borrajo, R. J. J. Williams, and F. M. Clara, *J. Appl. Polym. Sci.*, **28**, 485 (1983).

Received November 20, 1983

Accepted December 12, 1983